PHILOSOPHICAL TRANSACTIONS OF THE ROYAL SOCIETY A

Phil. Trans. R. Soc. A (2006) **364**, 611–622
doi:10.1098/rsta.2005.1726
Published online 24 January 2006

Inverse free electron lasers and laser wakefield acceleration driven by CO_2 lasers

By W. D. Kimura[1,*], N. E. Andreev[4], M. Babzien[2], I. Ben-Zvi[2], D. B. Cline[3], C. E. Dilley[1], S. C. Gottschalk[1], S. M. Hooker[6], K. P. Kusche[2], S. V. Kuznetsov[4], I. V. Pavlishin[2], I. V. Pogorelsky[2], A. A. Pogosova[4], L. C. Steinhauer[7], A. Ting[8], V. Yakimenko[2], A. Zigler[5] and F. Zhou[3]

[1]*STI Optronics, Inc., Bellevue, WA 98004-1495, USA*
[2]*Brookhaven National Laboratory, Upton, NY 11973, USA*
[3]*University of California at Los Angeles, Los Angeles, CA 90095, USA*
[4]*Institute for High Energy Densities, Russian Academy of Sciences, Moscow 125412, Russia*
[5]*Racah Institute of Physics, The Hebrew University, Jerusalem 91904, Israel*
[6]*University of Oxford, Oxford OX1 3PU, UK*
[7]*Redmond Plasma Physics Laboratory, University of Washington, Redmond, WA 98052, USA*
[8]*Naval Research Laboratory, Washington, DC 20375, USA*

The staged electron laser acceleration (STELLA) experiment demonstrated staging between two laser-driven devices, high trapping efficiency of microbunches within the accelerating field and narrow energy spread during laser acceleration. These are important for practical laser-driven accelerators. STELLA used inverse free electron lasers, which were chosen primarily for convenience. Nevertheless, the STELLA approach can be applied to other laser acceleration methods, in particular, laser-driven plasma accelerators. STELLA is now conducting experiments on laser wakefield acceleration (LWFA). Two novel LWFA approaches are being investigated. In the first one, called pseudo-resonant LWFA, a laser pulse enters a low-density plasma where nonlinear laser/plasma interactions cause the laser pulse shape to steepen, thereby creating strong wakefields. A witness *e*-beam pulse probes the wakefields. The second one, called seeded self-modulated LWFA, involves sending a seed *e*-beam pulse into the plasma to initiate wakefield formation. These wakefields are amplified by a laser pulse following shortly after the seed pulse. A second *e*-beam pulse (witness) follows the seed pulse to probe the wakefields. These LWFA experiments will also be the first ones driven by a CO_2 laser beam.

Keywords: laser acceleration; laser wakefield acceleration; inverse free electron laser; CO_2 laser; microbunch

* Author for correspondence (wkimura@stioptronics.com).

One contribution of 15 to a Discussion Meeting Issue ‘Laser-driven particle accelerators: new sources of energetic particles and radiation’.

1. Introduction

Research in plasma-based electron accelerators driven by intense laser light has demonstrated ultrahigh acceleration gradients exceeding 1 GeV m^{-1} (Leemans 2004). Among the various schemes being investigated, laser wakefield acceleration (LWFA) is a particularly promising one (Gorbunov & Kirsanov 1987). In LWFA, the laser beam is focused into a plasma where it generates a plasma wave (wakefield), which can travel close to the speed of light c. Electrons properly phased or 'trapped' within the electric field of the wakefield can be accelerated to high energies. Hence, this process is fundamentally similar to acceleration using microwaves in waveguides or direct acceleration by the laser field as occurs in inverse free electron lasers (IFEL) (Courant *et al.* 1985). A key difference is the much higher acceleration gradients that are possible with LWFA.

A practical accelerator requires more than just high acceleration gradients—it must have acceptable electron beam (e-beam) quality. For example, the electrons must have a narrow energy spread (i.e. monoenergetic) as they are accelerated. Furthermore, a useful e-beam charge implies an appreciable number of electrons must be trapped together when they are accelerated. Finally, these characteristics must be maintained along the entire length of the accelerator, which may consist of multiple acceleration stages.

In conventional microwave-driven accelerators, these needed e-beam characteristics are achieved by creating microbunches of electrons that are trapped within the travelling microwave field. This same process was demonstrated experimentally for waves at optical frequencies in the staged electron laser acceleration (STELLA) experiment (Kimura *et al.* 2004*a*). STELLA used an IFEL modulator driven by a CO_2 laser beam to create a train of microbunches that were subsequently trapped and accelerated in a second IFEL. The microbunches were approximately 1 μm long and separated by 10.6 μm (the laser beam wavelength). Trapping efficiencies up to approximately 80% and energy spreads of the accelerated electrons as low as 0.36% (1σ) were demonstrated (Kimura *et al.* 2004*b*).

Hence, STELLA demonstrated at optical wavelengths several key attributes needed by a practical laser-driven accelerator. These are: (i) microbunch formation with bunch lengths a fraction of the accelerating optical wavelength; (ii) staging between two laser-driven devices, whereby the microbunches produced by the first device are rephased properly with the accelerating field in the second device; (iii) efficient trapping of the microbunches within this accelerating field; and (iv) monoenergetic acceleration of the trapped electrons.

The success of the STELLA effort laid the groundwork for applying the basic STELLA approach to LWFA. Instead of an IFEL, an LWFA-driven modulator can be used to create microbunches, which can be trapped and accelerated in subsequent LWFA stages. While simple in concept, its practical implementation faces many challenges because of fundamental differences between LWFA and IFEL.

This paper describes the STELLA-laser wakefield (STELLA-LW) program whose goal is to use LWFA to demonstrate microbunch formation, staging, trapping and monoenergetic acceleration. To accomplish this requires devising methods for sufficiently controlling the wakefield formation process in each

LWFA stage so that the microbunches can be reliably rephased with the wakefields. Towards that aim, the STELLA-LW program is exploring two novel approaches called pseudo-resonant LWFA and seeded self-modulated LWFA (SM-LWFA), which are variants of the standard LWFA methods. Both offer the potential for creating strong wakefields that may be also more suitable for staging, i.e. the phase of the wakefields can be accurately controlled from shot to shot.

Section 2 briefly reviews the STELLA IFEL experimental results in order to provide a reference for the STELLA-LW experiment. Section 3 describes the two novel LWFA approaches and presents the model predictions. Conclusions are given in §4.

2. Review of STELLA IFEL experiment

Details of the STELLA IFEL experiment have been published elsewhere (Kimura *et al.* 2004*a*). It is located at the Brookhaven National Laboratory Accelerator Test Facility (ATF). The first step in the STELLA approach is the creation of microbunches by modulating the energy of the *e*-beam. As mentioned, this was done using a 'modulator' or 'buncher' IFEL. In an IFEL, co-propagating electron and laser beams pass through the gap of a device called a wiggler or undulator consisting of a pair of periodic magnet arrays facing each other. The undulator causes the electron trajectory to oscillate in the same plane as the laser beam electric field. Net energy exchange between the laser electric field and the electrons occurs when the resonant condition is satisfied (van Steenbergen *et al.* 1996)

$$\gamma^2 = \frac{\lambda_\mathrm{w}}{2\lambda_\mathrm{L}}\left(1 + \frac{K^2}{2}\right), \tag{2.1}$$

where γ is the Lorentz factor, λ_w is the undulator wavelength, λ_L is the laser wavelength, $K = eB_\mathrm{o}\lambda_\mathrm{w}/2\pi mc$, e is the electron charge, B_o is the peak magnetic field and m is the electron rest mass. Higher energy exchange is possible if the undulator is tapered, e.g. the gap or magnetic period becomes smaller along the magnet array (Kroll *et al.* 1981).

During the STELLA IFEL experiment, a 45 MeV *e*-beam with a single macrobunch length of approximately 3 ps (physical length is approx. 900 μm) overlaps inside the modulator IFEL with a CO_2 laser beam ($\lambda_\mathrm{L} = 10.6$ μm, pulse length is approx. 180 ps). Since the macrobunch is much shorter than the laser pulse length, the electrons experience approximately a uniform peak electric field. However, since the laser wavelength is much shorter than the macrobunch, the electrons within the macrobunch experience different phases of the electric field. This results in sinusoidal modulation of the electron energies within the macrobunch with a period equal to λ_L. Figure 1 shows the measured modulated energy spectrum from the IFEL. The symmetric double peaks are indicative of sinusoidal modulation.

When these modulated electrons continue travelling downstream, the faster (i.e. more energetic) electrons catch up in longitudinal position with the slower (i.e. less energetic) electrons. This causes the electrons to bunch together

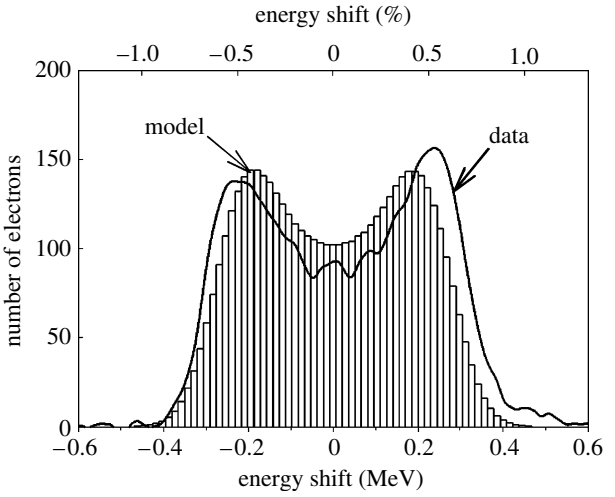

Figure 1. Typical energy modulation spectrum from STELLA IFEL experiment of the *e*-beam after passing through the first 'modulator' IFEL. Data: solid curve; model: histogram.

creating microbunches. This bunching process can also be accomplished in a shorter distance by passing the modulated *e*-beam through a magnetic chicane. The chicane causes the electrons to travel through a V-shaped trajectory, in which the faster electrons traverse a shorter path than the slower ones, thereby causing the electrons to bunch together. The STELLA experiment demonstrated microbunching with either a drift space (Kimura *et al.* 2001) or a chicane (Kimura *et al.* 2004*a*).

Thus, in every optical period a single microbunch is formed. Within the 900 μm long macrobunch there are approximately 85 such optical periods, thereby creating a train of 85 microbunches. These microbunches must be trapped and accelerated in subsequent acceleration stages. This is the second step of the STELLA process.

The microbunch train is sent into a second 'accelerator' IFEL, which utilizes a tapered undulator and is driven by much higher laser intensity to accelerate the microbunches. The microbunches are properly phased with the laser field in the second IFEL by adjusting the magnetic field of the chicane.

Figure 2 shows the experimentally measured energy spectrum of the electrons exiting the second IFEL along with the model prediction. Approximately 80% of the electrons have been trapped with a 1σ energy spread of approximately 1.2%. Other data had energy spreads as low as 0.36% (1σ). Additional modelling (Kimura *et al.* 2004*c*) shows it is possible to continue accelerating the trapped electrons to even higher energies (e.g. 1 GeV) in subsequent IFEL acceleration stages.

3. Description of STELLA-LW experiment

(*a*) *Review of experimental approach*

Like STELLA IFEL, the first task for the STELLA-LW experiment is the creation of microbunches by modulation of the *e*-beam using a 'modulator'

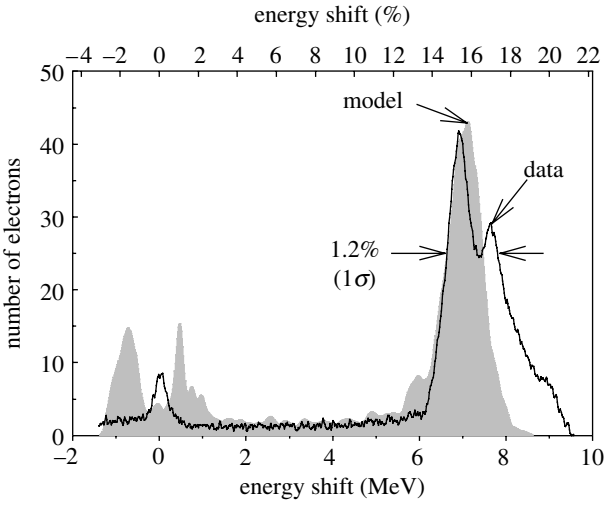

Figure 2. Example from STELLA IFEL experiment of the measured *e*-beam energy spectrum (solid line) compared with the model prediction (histogram) after the microbunches from the first 'modulator' IFEL pass through the second 'accelerator' IFEL.

LWFA. Although an IFEL could create microbunches to feed into an LWFA device, the spacing of the microbunches will not, in general, match the wakefield period (i.e. plasma wavelength λ_p), because typically $\lambda_L \neq \lambda_p$. There are two standard approaches for implementing LWFA. The first is called resonant LWFA where the laser beam driving the plasma has a pulse length $\tau_L \sim \lambda_p/2c$. Wakefields are excited because the laser pulse's primary Fourier component matches the plasma frequency. The plasma wavelength is related to the plasma density n_e via

$$\lambda_p(\mu\text{m}) = \frac{\left(3.34 \times 10^{10}\right)}{\sqrt{n_e(\text{cm}^{-3})}}. \tag{3.1}$$

For the STELLA-LW experiment, we intend to use the ATF CO_2 laser as the laser source. Driving the LWFA process using 10 μm laser light has not been demonstrated before, although there are potential advantages (Pogorelsky 1998) of using 10 μm light instead of the order of 1 μm laser light that has been typically used by others. The ATF laser is capable of delivering more than 1 TW of peak power in pulse lengths ultimately as short as 2–3 ps (present pulse length is approx. 15 ps). If $\tau_L = 2$ ps, then at resonance $\lambda_p \sim 1.2$ mm and $n_e \sim 7 \times 10^{14}\,\text{cm}^{-3}$. It would be very difficult to obtain such a low plasma density. This implies that the 2 ps ATF CO_2 laser pulse is not short enough to drive resonant LWFA.

Another LWFA approach is called SM-LWFA, in which the laser pulse length is intentionally much longer than $\lambda_p/2c$ (Andreev *et al.* 1992; Sprangle *et al.* 1992; Antonsen *et al.* 1992). This permits the laser electric field to feed energy into a wakefield via forward Raman scattering and/or a self-modulation instability. Much higher gradients are possible using SM-LWFA. However, this mechanism starts from noise and becomes a highly nonlinear process, which may compromise the possibility of controlling the wakefield phase. In addition, SM-LWFA model

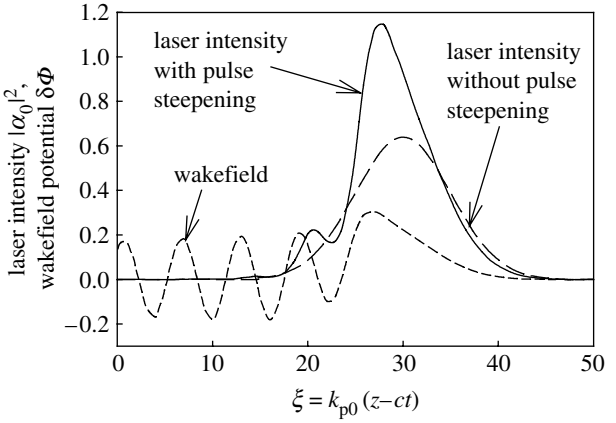

Figure 3. Sample model prediction for pseudo-resonant LWFA from Andreev *et al.* (2003). Plotted is the laser pulse intensity (with and without the pulse steepening effect) and change in wakefield potential $\delta\Phi$ on axis at propagation distance $z=5.5$ cm into the plasma versus the dimensionless coordinate $\xi = k_{p0}(z-ct)$, where $k_{p0}=(4\pi\, e^2\, n_e/m)^{1/2}/c$.

simulations for the ATF CO_2 laser conditions indicate transverse wakefields are predominately generated rather than longitudinal wakefields, which are responsible for accelerating the electrons. Thus, conventional SM-LWFA is also not feasible with the ATF CO_2 laser.

Hence, demonstration of an LWFA modulator at the ATF requires devising new schemes for initiating the LWFA process within the constraints of the ATF CO_2 laser capabilities. Fortunately, two such schemes have been developed and are described next.

(*b*) *Pseudo-resonant LWFA*

The first scheme is called pseudo-resonant LWFA (Andreev *et al.* 2003). The key concept in this process is that a laser pulse focused in the plasma will undergo nonlinear interaction with the plasma. If the laser pulse is long enough (a few plasma wavelengths or longer), this nonlinear interaction gives rise to the SM-LWFA effect. However, for shorter pulses, the nonlinear processes cause steepening of the laser pulse whereby the trailing edge of the pulse shortens and the peak increases (Sprangle *et al.* 2000). The growth of the laser pulse amplitude in the back of the pulse with a sharp drop after the peak is due to self-phase modulation and group velocity dispersion (Esarey *et al.* 2000; Sprangle *et al.* 2000). This pulse steepening makes the laser pulse act as if it has components of much shorter length that can excite the resonant LWFA interaction. Model simulations show that strong wakefields can be generated even though the incoming laser pulse length is several times longer than the resonance length $\lambda_p/2c$.

Figure 3 illustrates the pseudo-resonant LWFA effect (Andreev *et al.* 2003). Shown is the LWFA model prediction for the anticipated conditions of the ATF TW CO_2 laser (i.e. approx. 2 ps pulse length, 5 J per pulse) at 5.5 cm into the plasma and a plasma density $n_e=1.1\times10^{16}\,\mathrm{cm}^{-3}$. Plotted is the laser intensity and the wakefield potential $\delta\Phi$, where $\delta\Phi=\Phi-1$ and Φ is the scalar potential of

the wakefield normalized by e/mc^2. In the figure, the leading edge of the laser pulse is on the right-hand side.

In figure 3, the laser intensity without pulse steepening has a symmetric Gaussian shape—the same shape it had before entering the plasma. With pulse steepening the laser intensity at the trailing edge of the pulse becomes steeper and its peak intensity increases. Clearly, this steep trailing edge is associated with the formation of the first plasma wake, which has a much shorter wavelength than the initial Gaussian laser pulse. Note that the formation of this first wake leads to a slight modulation of the laser beam intensity profile at the end of the laser pulse. This modulation is in fact the beginning of the self-modulation process that would occur if the laser pulse were much longer as in SM-LWFA. But, in our case, the laser pulse terminates before SM-LWFA can begin in earnest. Nonetheless, strong wakefields are generated that are comparable in strength to ones generated by SM-LWFA. Electric field gradients of the order of 1 GV m^{-1} are predicted for the ATF conditions.

Thus, the pseudo-resonant LWFA process shares characteristics of both resonant LWFA and SM-LWFA. Like resonant LWFA, the point of wakefield formation is tied closely to the laser pulse shape, i.e. at the steepened trailing edge of the laser pulse. The wakefield does not start from noise as it does in SM-LWFA. This is important because it implies the possibility of controlling the wakefield phase by controlling the arrival time of the laser pulse.

One can consider how pulse-to-pulse variations might then affect the wakefield phase. Suppose the laser pulse length varies by, say, 10%, then the relative wakefield phase shift will be approximately $0.1c\tau_L/\lambda_p$, which is about 10%, since the laser pulse length is of the order of the plasma wavelength in the pseudo-resonant regime. Predicting changes in the wakefield phase with variations in the laser pulse shape, e.g. the steepness of the trailing edge, would require more extensive modelling because the processes are nonlinear.

(*c*) *Seeded SM-LWFA*

The second method for generating appreciable wakefields using the ATF CO_2 laser is called seeded SM-LWFA. This idea was originally introduced as stimulated LWFA (Steinhauer *et al.* 2002). The basic concept is to use either a short *e*-beam pulse or laser pulse to act as a seed pulse to initiate wakefield formation via resonant plasma wakefield acceleration (PWFA) or LWFA, respectively. These wakefields are then amplified in strength via SM-LWFA by sending the CO_2 laser pulse immediately after the seed pulse. An additional benefit of this method is that the wakes are initially formed via resonant PWFA or resonant LWFA. This should produce more controllable wakes, and, hence, this method may permit creation of both strong and controllable wakefields.

Using a magnetic bunch compressor on the linac beamline, the ATF is able to create electron bunches that are theoretically estimated to be approximately 200 fs in duration. This sub-picosecond *e*-beam pulse can be used as the resonant seed pulse.

In typical LWFA experiments, the laser pulse creates the wakefields and then an *e*-beam follows shortly thereafter to probe the wakefields. If a seed *e*-beam pulse initiates the wakefield formation, a second witness *e*-beam pulse will be needed to follow the seed pulse and probe the wakefields amplified by the laser

pulse. This means the linac must provide two *e*-beam pulses separated by a short time interval. Fortunately, the ATF has already demonstrated multiple *e*-beam pulses from its photocathode. Moreover, recent tests have demonstrated the ability to send two *e*-beam pulses through the bunch compressor. The first pulse is phased for compression; the second pulse lags behind and is not compressed. The pulses are phased on the radio-frequency cycle so that their energy difference is approximately 1 MeV. Maintaining similar energies of the two pulses is important in order for the beamline optics to have approximately the same affects on the two pulses. This is especially critical because of the need for tight focusing of the *e*-beam pulses into a capillary discharge, which will be used as the plasma source (Kimura *et al.* 2005).

The LWFA model as described by Andreev *et al.* (2003) was modified to incorporate both seed and witness *e*-beam pulses. Equations (3.2)–(3.5) are reproductions of eqns (4)–(7) in Andreev *et al.* (2003), except for the addition of a new term $\boldsymbol{j}_\mathrm{b}$ in equation (3.4) that represents the current density of the seed *e*-beam bunch.

$$\frac{\partial \boldsymbol{p}}{\partial t} = e\boldsymbol{E} - mc^2\nabla\gamma, \tag{3.2}$$

$$\frac{\partial n}{\partial t} + \nabla\cdot(n\boldsymbol{v}) = 0, \tag{3.3}$$

$$\frac{\partial \boldsymbol{E}}{\partial t} = -4\pi en\boldsymbol{v} + c\nabla\times\boldsymbol{B} - 4\pi\boldsymbol{j}_\mathrm{b}, \tag{3.4}$$

$$\nabla\times\boldsymbol{E} = -\frac{1}{c}\frac{\partial \boldsymbol{B}}{\partial t}, \tag{3.5}$$

where $\boldsymbol{E}$ and $\boldsymbol{B}$ are the electric field and magnetic flux in the plasma, respectively; $\gamma = [1 + (p/mc)^2 + (1/2)|a|^2]^{1/2}$; n is the plasma electron density; $\boldsymbol{p}$ and $\boldsymbol{v}$ are the electron momentum and velocity, respectively; and a is the dimensionless envelope amplitude of the laser pulse (Andreev *et al.* 2003). These equations describe the slowly varying motions and fields in the plasma. We assume the seed *e*-beam is relativistic with a current that is some given function of time and space, e.g. Gaussian.

Using the same dimensionless variables, ξ and ρ, as defined by Andreev *et al.* (2003), the simplified linearized equation for the wakefield potential variation $\delta\Phi$ has the form

$$\left\{\left(\frac{\partial^2}{\partial\xi^2} + \nu_0\right)(\Delta_\perp - \nu_0) - \frac{\partial \ln(\nu_0(r))}{\partial\rho}\frac{\partial^2}{\partial\xi^2}\frac{\partial}{\partial\rho}\right\}\delta\Phi = \nu_0\left[(\Delta_\perp - \nu_0)\frac{|a|^2}{4} - N_\mathrm{b}\right], \tag{3.6}$$

where ν_0 is the normalized electron background density in the plasma channel, N_b is the normalized seed electron bunch density and $\Delta_\perp$ is the transverse part of the Laplacian operator. All other equations have the same form as given by Andreev *et al.* (2003).

Table 1 lists the important parameter values assumed in the upgraded model. The conventions for describing the *e*-beam and laser beams are as follows. The laser

Table 1. Laser, plasma and *e*-beam parameters used in seeded SM-LWFA simulations.

parameter	value
laser wavelength, λ_L	10.6 μm
laser pulse duration, τ_L	8.44 ps
laser peak power, P_L	0.5 TW
laser pulse energy, E_L	5.3 J
laser beam focus radius, w_0	111 μm
laser beam Rayleigh range, z_R	3.64 mm
normalized laser field strength, a_0	0.462
plasma density on axis, n_e	0.89×10^{17} cm^{-3}
e-beam energy (seed and witness), E_{inj}	64 MeV
seed *e*-beam pulse charge	199 pC
seed *e*-beam pulse length, $\tau_{e\text{-seed}}$	118 fs
seed *e*-beam focus size at capillary (1σ)	50 μm
witness *e*-beam intrinsic energy spread (%)	0.05
witness *e*-beam pulse length, $\tau_{e\text{-witness}}$	1.23 ps
witness *e*-beam focus size at capillary (1σ)	20 μm

beam amplitude a or field strength is

$$a(r, z = 0, t) = a_0 \exp\left[-\frac{r^2}{w_0^2} - \frac{(t-t_0)^2}{\tau_L^2}\right], \tag{3.7}$$

and the *e*-beam charge distribution is

$$i(r, z = 0, t) = i_0 \exp\left[-\frac{r^2}{2\sigma_e^2} - \frac{(t-t_0)^2}{2\tau_e^2}\right], \tag{3.8}$$

where $\tau_e \equiv \tau_{e\text{-seed}}$ and $\tau_e \equiv \tau_{e\text{-witness}}$ for the seed and witness *e*-beam pulses, respectively. These conventions were adopted because of their common usage within the laser and accelerator communities, respectively. For example, w_0 is the usual waist of the laser beam focus, whereas σ_e is the r.m.s. size of the *e*-beam.

There are differences in the parameter values in table 1 and those assumed for the pseudo-resonant LWFA results shown in figure 3. Most noteworthy is the plasma density on axis is almost 10 times larger (0.89×10^{17} cm^{-3}) because of the availability of the sub-picosecond seed pulse. This higher density should be easier to achieve using gas-filled capillary discharges that will be utilized during the STELLA-LW experiment (Kimura *et al.* 2005).

Figure 4 is a sample prediction for the seeded SM-LWFA experiment. Plotted is the laser field parameter with and without the seed *e*-beam pulse present. In the absence of the seed, the laser pulse shape is Gaussian and no wakefields are produced. With the seed present, wakefields begin to form as seen by the increase of the wakefield potential immediately trailing the seed pulse. At the same time a modulation on the envelope of the laser field begins to appear, which is evidence of a self-modulation interaction between the wakefields and the laser field. This enhances the wakefields produced by the seed.

Figure 5 shows the resulting energy spectrum of the witness *e*-beam pulse (see lower right-hand side of figure 4) as a function of delay time τ_d after the seed pulse for an acceleration length of 2 mm. After a delay of approximately 9 ps,

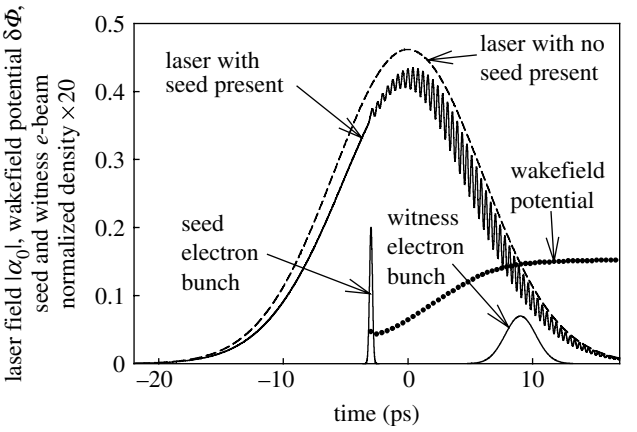

Figure 4. Sample model prediction for seeded SM-LWFA. Plotted is the laser field parameter $a_0(r=0)$ and wakefield potential $\delta\Phi(r=0)$ as a function of time, where the delay time between the peak of the seed e-beam pulse and the laser pulse is $\tau_d = 2.97$ ps and the distance in the plasma is 2.62 mm. Other parameters are listed in table 1. Also plotted is an example of the witness e-beam pulse position.

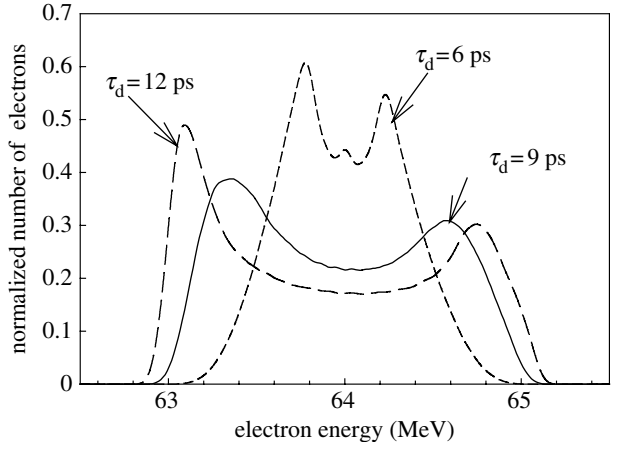

Figure 5. Model prediction for electron energy spectrum of witness e-beam pulse shown in figure 4 as a function of time delay τ_d between the seed and witness e-beam pulses. For this simulation, the plasma acceleration length is 2 mm. Other parameters are listed in table 1.

a double-peak modulation spectrum is seen with a width of approximately ± 1 MeV (cf. figure 1). This amount of modulation is well suited for forming microbunches. Hence, this particular configuration could serve as the LWFA modulator.

Changing the time delay between the seed and laser pulse, and using longer acceleration lengths permits achieving higher energy gains. For example, the model predicts 6 MeV energy gain over 3 mm plasma length corresponding to 2 GeV m^{-1} acceleration gradient. Thus, a second LWFA device based on this configuration for seeded SM-LWFA could serve as the 'accelerator' portion of a staged LWFA system.

4. Conclusion

Preparations are currently underway at the ATF to perform seeded SM-LWFA experiments utilizing the current capabilities of the ATF CO_2 laser and linac bunch compressor. (More details of the plasma sources to be used are described in Kimura *et al.* 2005.) Once the ATF CO_2 laser has been upgraded to output 2–3 ps laser pulses, pseudo-resonant LWFA experiments can be performed. Both methods may enable creation of a suitable LWFA modulator for making microbunches. These microbunches can be subsequently trapped and accelerated in a second LWFA acceleration stage. This second LWFA stage would be investigated in future phases of the STELLA-LW experiment.

This work was supported by the US Department of Energy, grant nos. DE-FG02-04ER41294, DE-AC02-98CH10886 and DE-FG03-92ER40695.

References

Andreev, N. E., Gorbunov, L. M., Kirsanov, V. I., Pogosova, A. A. & Ramazashvili, R. R. 1992 Resonant excitation of wakefields by a laser pulse in a plasma. *JETP Lett.* **55**, 571–577.

Andreev, N. E., Kuznetsov, S. V., Pogosova, A. A., Steinhauer, L. C. & Kimura, W. D. 2003 Modeling of laser wakefield acceleration at CO_2 laser wavelengths. *Phys. Rev. ST Accel. Beams* **6**, 041 301. (doi:10.1103/PhysRevSTAB.6.041301)

Antonsen Jr, T. M. & Mora, P. 1992 Self-focusing and Raman scattering of laser pulses in tenuous plasmas. *Phys. Rev. Lett.* **69**, 2204. (doi:10.1103/PhysRevLett.69.2204)

Courant, E. D., Pellegrini, C. & Zakowicz, W. 1985 High-energy inverse free-electron-laser accelerator. *Phys. Rev. A* **32**, 2813–2823. (doi:10.1103/PhysRevA.32.2813)

Esarey, E., Schroeder, C. B., Shadwick, B. A., Wurtele, J. S. & Leemans, W. P. 2000 Nonlinear theory of nonparaxial laser pulse propagation in plasma channels. *Phys. Rev. Lett.* **84**, 3081. (doi:10.1103/PhysRevLett.84.3081)

Gorbunov, L. M. & Kirsanov, V. I. 1987 Excitation of plasma waves by an electromagnetic wave packet. *Sov. Phys. JETP* **66**, 290–294.

Kimura, W. D. *et al.* 2001 First staging of two laser accelerators. *Phys. Rev. Lett.* **86**, 4041–4043. (doi:10.1103/PhysRevLett.86.4041)

Kimura, W. D. *et al.* 2004*a* Detailed experimental results for high-trapping efficiency and narrow energy spread in a laser-driven accelerator. *Phys. Rev. ST Accel. Beams* **7**, 091 301. (doi:10.1103/PhysRevSTAB.7.091301)

Kimura, W. D. *et al.* 2004*b* First demonstration of high-trapping efficiency and narrow energy spread in a laser-driven accelerator. *Phys. Rev. Lett.* **92**, 054 801. (doi:10.1103/PhysRevLett.92.054801)

Kimura, W. D., Musumeci, P., Quimby, D. C., Gottschalk, S. C. & Pellegrini, C. 2004*c* Conceptual design for a 1-GeV IFEL accelerator. In *Advanced accelerator concepts* (ed. V. Yakimenko). *AIP Conf. Proc. No. 737*, pp. 251–257. New York: American Institute of Physics.

Kimura, W. D. *et al.* 2005 Pseudo-resonant laser wakefield acceleration driven by 10.6 μm laser light. *IEEE Trans. Plasma Sci.* **33**, 3–7. (doi:10.1109/TPS.2004.841173)

Kroll, N. M., Morton, P. L. & Rosenbluth, M. N. 1981 Free-electron lasers with variable parameter wigglers. *IEEE J. Quantum Electron.* **QE-17**, 1436–1468. (doi:10.1109/JQE.1981.1071285)

Leemans, W. 2004 Advances in laser driven accelerator R&D. In *Advanced accelerator concepts* (ed. V. Yakimenko). *AIP Conf. Proc. No. 737*, pp. 11–28. New York: American Institute of Physics.

Pogorelsky, I. V. 1998 Prospects for laser wakefield accelerators and colliders using CO_2 laser drivers. *Nucl. Instrum. Methods Phys. Res. A* **410**, 524–531. (doi:10.1016/S0168-9002(98)00160-0)

Sprangle, P., Esarey, E., Krall, J. & Joyce, G. 1992 Propagation and guiding of intense laser pulses in plasmas. *Phys. Rev. Lett.* **69**, 2200. (doi:10.1103/PhysRevLett.69.2200)

Sprangle, P., Hafizi, B., Penano, J. R., Hubbard, R. F., Ting, A., Zigler, A. & Antonsen Jr, M. T. 2000 Stable laser-pulse propagation in plasma channels for GeV electron acceleration. *Phys. Rev. Lett.* **24**, 5110–5112. (doi:10.1103/PhysRevLett.85.5110)

Steinhauer, L. C., Kimura, W. D. & Agarwal, R. N. 2002 Stimulated laser wakefield acceleration. In *Proc. Int. Conf. on Lasers 2001* (ed. V. J. Corcoran & T. A. Corcoran), pp. 159–163. Mclean, VA: STS Press.

van Steenbergen, A., Gallardo, J., Sandweiss, J., Fang, J.-M., Babzien, M., Qiu, X., Skaritka, J. & Wang, X.-J. 1996 Observation of energy gain at the BNL inverse free-electron-laser accelerator. *Phys. Rev. Lett.* **77**, 2690–2693. (doi:10.1103/PhysRevLett.77.2690)